

# Isotope purification induced reduction of spin relaxation and spin coherence times in semiconductors

Oscar Balancea-Lindvall,<sup>1</sup> Matthew Travis Eiles,<sup>2</sup> Nguyen Tien Son,<sup>1</sup> Igor A. Abrikosov,<sup>1</sup> and Viktor Ivády<sup>1,2,\*</sup>

<sup>1</sup>*Department of Physics, Chemistry and Biology, Linköping University, SE-581 83 Linköping, Sweden*

<sup>2</sup>*Max-Planck-Institut für Physik komplexer Systeme, Nöthnitzer Street 38, D-01187 Dresden, Germany*

(Dated: May 12, 2022)

Paramagnetic defects and nuclear spins are often the major sources of decoherence and spin relaxation in solid-state qubits realized by optically addressable point defect spins in semiconductors. It is commonly accepted that a high degree of depletion of nuclear spins can enhance the coherence time by reducing magnetic noise. Here we show that the isotope purification beyond a certain optimal level becomes contra-productive, when both electron and nuclear spins are present in the vicinity of the qubits. Using state-of-the-art numerical tools and considering the silicon vacancy qubit in various spin environments, we demonstrate that the coupling to spin-1/2 point defects in the lattice can be significantly enhanced by isotope purification. The enhanced coupling shortens the spin relaxation time that in turn may limit the coherence time of spin qubits. Our results can be straightforwardly generalized to triplet point defect qubits, such as the NV center in diamond and the divacancy in SiC.

## INTRODUCTION

Point defect qubits in semiconductors exhibit long coherence time at cryogenic and room temperature.[1–3] Combining this feature with advanced magneto-optical control of the qubit state has enabled these systems to become the leading contender in several areas of quantum technology.[4–6] The properties of point defect qubits depend to a very large degree on the host material. In particular, magnetic fluctuations in the local spin environment of the defects can profoundly influence the defect's coherence time, in most cases reducing it by several orders of magnitude from the theoretical upper limit set by the spin relaxation time.[1, 7] As a result, a strategy of chemical and isotope purification in the host material is commonly pursued in order to enhance the coherence time of the point defect qubits. It is believed that this strategy can be applied in most of the cases.[1, 7–12]

In this Letter, we report on a counterintuitive effect that emerges when both electron and nuclear spins are present in the vicinity of the qubits. In particular, we show that isotope purification leads to a significant reduction of the spin relaxation time, due to enhanced cross relaxation effects with other paramagnetic defects of similar fine structure. This effect in turn sets a reduced upper limit for the coherence time. We study the phenomenon numerically for the quartet silicon vacancy center in SiC, where the consequences may be of high importance. Our results can be easily extended to other spin defects, such as the NV center in diamond and the divacancy in SiC.

The negatively charged silicon vacancy in SiC exhibits a quartet ground state spin with long coherence time[3, 13]. This high spin state has been utilized in quantum sensing applications[14–21] and to implement a room temperature maser [22]. Furthermore, the defect's favourable optical properties[23, 24] and advanced fabrication capabilities[25–27] make it potentially interesting for novel near-infrared quantum information processing applications.[22, 26–32] In 4H-SiC, the V1 and V2 photoluminescence lines and the Tv1-

Tv2 electron spin resonance (ESR) signals[33–37] are related to the negatively charged silicon vacancy. The V1 and V2 center were assigned to the  $h$  and  $k$  silicon vacancy configurations, respectively, by comparing with first principles results[38, 39]. In our numerical studies we consider the V2 center, which is the most often studied configuration.

There are two main ingredients of the environmental spin bath in SiC. Natural samples include 4.7%  $^{29}\text{Si}$  and 1.1%  $^{13}\text{C}$  spin-1/2 nuclear spins. In addition, the structure of the host material incorporates various paramagnetic defects and impurities, whose concentrations may vary over several orders of magnitudes depending on the growth conditions, after growth sample preparation, and nano-scale fabrication. Here, we consider the most common intrinsic spin-1/2 defects, such as carbon vacancy and carbon antisite-vacancy pair whose concentration can reach  $10^{15} \text{ cm}^{-3}$  in HPSI 4H-SiC.[30, 40] We note that this value may increase by 2-3 orders of magnitude due to irradiation and implantation that are frequently used techniques to create silicon vacancy qubits.

In our study, we divide the complex ground state spin Hamiltonian of the quartet silicon vacancy-environmental spin bath system into two parts,

$$H = H_1 + H_2, \quad (1)$$

where  $H_1$  and  $H_2$  describe one and two-spin interaction terms, respectively.  $H_1$  includes the zero-field splitting (ZFS) interaction of the quartet silicon vacancy and Zeeman terms of all the spins in the system,

$$H_1 = D \left( S_{0,z}^2 - \frac{5}{4} \right) + g_{3\parallel} \mu_B \frac{S_{0,+}^3 - S_{0,-}^3}{4i} B_z + g_e \mu_B \sum_{j=0}^M S_{j,z} B_z + \mu_N \sum_{k=1}^N g_{N,k} I_{k,z} B_z, \quad (2)$$

where  $S_{j,z}$  is the  $z$  component of the electron spin operator vector  $\mathbf{S}_j$  of defect  $j$ ,  $I_{k,z}$  is the  $z$  component of the nuclear spin operator vector  $\mathbf{I}_k$  of nucleus  $k$ ,  $g_e$  is the g-factor

of the electron,  $\mu_B$  is the Bohr magneton,  $g_{N,k}$  is the nuclear g-factor of either  $^{13}\text{C}$  or  $^{29}\text{Si}$ , and  $\mu_N$  is the nuclear magneton. Terms with  $j = 0$  index label the silicon vacancy spin, while  $j > 0$  indices label the doublet paramagnetic defects in the environment. The ZFS parameter  $D$  is equal to 35.0 MHz for the V2 silicon vacancy configuration.[38] The second term on the r.h.s. of Eq. (2) accounts for a non-vanishing higher order term of the Zeeman interaction of the quartet spin states in  $C_{3v}$  symmetry, where  $g_{3||} = 0.6$ . [16, 41] The second term in the Hamiltonian,  $H_2$  in Eq. (2), accounts for the hyperfine and the dipolar coupling of the spins,

$$H_2 = \sum_{j=0}^M \sum_{k=1}^N \mathbf{S}_j A_{jk} \mathbf{I}_k + \sum_{i=0}^M \sum_{j>i}^M \frac{\mu_0}{4\pi} \frac{g_e^2 \mu_B^2}{r_{ij}^3} (\mathbf{S}_i \mathbf{S}_j - 3(\mathbf{S}_i \mathbf{r}_{ij})(\mathbf{S}_j \mathbf{r}_{ij})) + \sum_{k=1}^N \sum_{l>k}^N \frac{\mu_0}{4\pi} \frac{g_{N,k} g_{N,l} \mu_N^2}{r_{kl}^3} (\mathbf{I}_k \mathbf{I}_l - 3(\mathbf{I}_k \mathbf{r}_{kl})(\mathbf{I}_l \mathbf{r}_{kl})), \quad (3)$$

where  $A_{jk}$  is the hyperfine tensor,  $\mathbf{r}_{ij}$  is the position vector pointing from spin  $i$  to spin  $j$ , and  $r_{ij} = |\mathbf{r}_{ij}|$ .  $A_{jk}$  for  $j > 0$  are mostly unknown as they depend on the paramagnetic defects found in the vicinity of the silicon vacancy. For simplicity, we consider only the hyperfine interaction of the silicon vacancy, i.e.  $A_{jk} = 0$  for  $j > 0$ . This approximation does not affect our qualitative results, however, our quantitative results are the most accurate for environmental paramagnetic defects of small hyperfine interactions, such the common carbon vacancy in SiC. The hyperfine coupling tensors  $A_{0k}$  are obtained from first principles density functional theory calculations in Ref. [42] and used here as well. Beyond 15 Å distance from the silicon vacancy, the Fermi contact term is neglected and only the dipolar hyperfine term is considered. Local inhomogeneities at the defect sites due to the hyperfine interaction are included in calculations as an effective magnetic field. Accordingly, the first term on the r.h.s. of Eq. (3) is approximated as  $H_{\text{inhomo}} = \Delta S_{0,z}$ , where  $\Delta = \sum_k A_{0k,z} \langle I_{k,z} \rangle$  is the inhomogeneous splitting, or the nuclear Overhauser field in other contexts. Here, the angular bracket represents expectation value, while  $A_z = \sqrt{A_{xz}^2 + A_{yz}^2 + A_{zz}^2}$ .

In order to numerically study the Hahn-echo coherence time ( $T_2$ ) of the quartet silicon vacancy spin in natural and isotope purified SiC, we employ the second order generalized cluster correlation expansion (gCCE2) method[43]. The converged models include  $M \approx 1000$  nuclear spins within a sphere of radius  $r_{\text{Bath}}$  around the qubit. For natural nuclear spin abundance models  $r_{\text{Bath}} = 50$  Å is used, while for lower abundances  $r_{\text{Bath}}$  is increased to keep the average number of environmental spins  $M$  fixed. Nuclear spin pairs are considered within the cut-off radius  $r_{\text{dip}} = 6.0$  Å. The ensemble coherence function is obtained by averaging over 500 randomly generated spin bath configurations and fitted with an  $A \exp(-(t/T_2)^n)$  function to obtain the Hahn-echo coherence

time  $T_2$ . To study the coherence properties of the silicon vacancy, the  $|+3/2\rangle$  and the  $|+1/2\rangle$  states are used to implement a qubit.

In order to quantify the dipolar spin relaxation time ( $T_1$ ) of the quartet silicon vacancy spin states in a bath of spin-1/2 electron spins, we utilize the method recently developed in Ref. [42] and briefly reviewed in Ref. [44]. The spin bath models consist of  $N = 32$  electron spins with varying concentration. We use the first order cluster approximation, which is suitable for an electron spin bath of short coherence time[42, 44]. The time step of the propagation is set to 1 ps, while the simulation time is optimized for the considered concentrations and vary between 0.05 and 1 ms. The coupling strength between the qubit and the spin bath spins are obtained in the point-spin density approximation, i.e. by using the second term on the r.h.s. of Eq. (3).

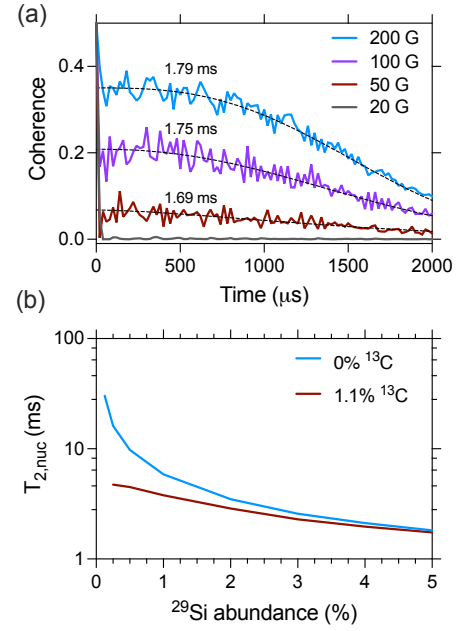


FIG. 1. Coherence of the quartet V2 center in a nuclear spin bath in SiC. (a) Decay of the coherence function at various magnetic field values for natural abundance of nuclear spins. The coherence time is provided for each curve. For  $B > 200$  G the coherence time saturates and takes the value of  $T_2 = 1.8$  ms. (b)  $^{29}\text{Si}$  abundance dependence of the saturated coherence time at  $B = 200$  G.

First, we study the coherence time of the V2 silicon vacancy qubit when *only nuclear spins* are included in the spin bath. The decay of the Hahn echo coherence function due to a surrounding nuclear spin bath of natural isotope abundance is depicted in Fig. 1(a). As can be seen, the coherence function decays on two different time scales. Due to the hyperfine interaction driven precession of the nuclear spins, see the first term on the r.h.s. of Eq. (3), the coherence function partially collapses at first with a time scale comparable with the inhomogeneous coherence time ( $T_2^*$ ). In contrast to the NV center, the coherence function does not recover later and no coherent

beatings can be observed. This irregular behaviour is due to the quartet spin state and further discussed in Ref. [45]. The long time scale decay, observable in Fig. 1(a), is due to the nuclear spin-nuclear spin interaction induced magnetic field fluctuations, see the last term on the r.h.s. of Eq. (3). The former effect dominates at small magnetic field values, i.e. at strong hyperfine coupling, while the latter effect dominates at high magnetic field values where the hyperfine interaction is suppressed by the Zeeman splitting of the nuclear spin states. The coherence time saturates above  $B = 200$  Gauss and takes the values of  $T_2 = 1.8$  ms for natural abundance of paramagnetic nuclei. The strength of the nuclear spin coupling and thus the saturated high magnetic field coherence time sensitively depend on the abundance of the nuclear spins. As expected, the  $T_2$  time significantly enhances as the nuclear spin bath is depleted, see Fig. 1(b). These results are in accordance with the anticipated behaviour of the system and previous results on the coherence time of the silicon vacancy.[45]

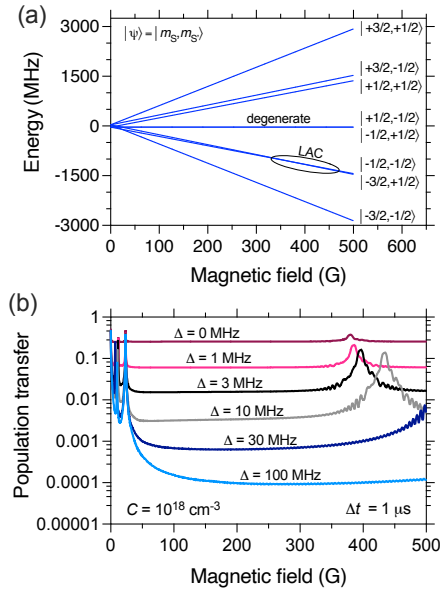


FIG. 2. Resonant coupling of a quartet electron spin and a doublet electron spin. (a) Energy levels of a quartet-doublet two electron spin system. The corresponding states are provided in the  $|m_S, m_{S'}\rangle$  basis, where the quantization axes is set parallel to the  $c$ -axis. (b) Thermalization of the quartet spin states in a bath of spin-1/2 electron spins. The vertical axis measures the amount of population transferred from the initial highly polarized  $m_S = +1/2$  state to the rest of the quartet states of the V2 center under a fixed evolution time of  $\Delta t = 1 \mu s$  in a bath of spin-1/2 electron spin of  $C = 10^{18} \text{ cm}^{-3}$  concentration. The figure depicts polarization transfer curves for various inhomogeneous splitting  $\Delta$  of the silicon vacancy states.

However, the host material includes not only nuclear spins but also other *electron spin defects* in the local environment of the qubits. In order to understand the behaviour of a quartet electron spin in a bath of spin-1/2 defects, we depict the magnetic field dependence of the energy levels of a quartet-doublet two electron spin system in Fig. 2(a). For large mag-

netic field values the Zeeman interaction is the strongest term in the spin Hamiltonian in Eq. (1). Due to the magnetic splitting of both the quartet and the doublet electron spins ( $g_e \approx 2$  for both spins), the energy levels form five distinct branches. The states that are included in the branches are labelled in Fig. 2(a). Note that each of the three innermost branches consist of a pair of states. These pairs include  $\Delta m_S = \pm 1$  and  $\Delta m_{S'} = \mp 1$  states of the quartet and the doublet states and can be effectively coupled by the  $S_{0,+}S'_{j,-} + S_{0,-}S'_{j,+}$  term of the second term in the r.h.s of Eq. (3). This interaction induces spin flip-flops of the electron spins, shortens the spin state lifetime, and thus limits the coherence time of the quartet silicon vacancy qubit states.

Since the dipolar coupling of the electron spins is generally small, any splitting of the spin states within the branches has a significant effect on the lifetime of the states. In this respect, it is noteworthy that the  $|+1/2, -1/2\rangle$  and the  $|-1/2, +1/2\rangle$  states are degenerate, when only ZFS and Zeeman interactions are taken into consideration, see Fig. 2(a). In contrast, the zero-field interaction splits the states in other branches. Due to the higher order terms of the Zeeman interaction of the quartet silicon vacancy, the states within a branch may cross each other, see for instance the region labelled by LAC in Fig. 2(a).

In order to study the thermalization of the silicon vacancy spin states in an electron spin bath, we simulate the population transfer from the initially highly polarized  $|+1/2\rangle$  state to the rest of the quartet spin states in Fig. 2(b). When the  $|+1/2, -1/2\rangle$  and  $|-1/2, +1/2\rangle$  states are degenerate, the initial population thermalizes within  $1 \mu s$  irrespective of the external magnetic field, see the uppermost curve in Fig. 2(b). On the other hand, by introducing an effective inhomogeneous magnetic field acting on the quartet spin state and causing a  $\Delta$  splitting in the  $m_S = \{-1/2, +1/2\}$  subspace of the quartet spin, the magnetic field independent component of the spin relaxation reduces drastically, indicating the elongation of the spin state lifetime at most magnetic field values. The remaining high population transfer peaks, below 50 G and at around 400-500 G in Fig. 2(b), are related to level anti-crossings (LACs) of the spin states that are studied in more details in Ref. [46]. Furthermore, we note that the reduced lifetime of the  $m_S = \{-1/2, +1/2\}$  state, beyond the theoretical expectations[19], has been recently reported in Ref. [47] and has been attributed to the coupling to spin-1/2 defects. These results indicate that the inhomogeneous splitting of the spin states plays a crucial role in elongating the spin state lifetime in an electron spin bath.

There are several different sources of local inhomogeneous fields that in principle could induce a splitting of the degenerate subspace of the coupled quartet-doublet spin states and suppress the mutual flip-flops of the spins. Hyperfine coupling is typically the strongest interaction that can give rise to local inhomogeneities on sub-nanometer scales. In order to quantify the hyperfine interaction induced inhomogeneity, we study the distribution of the hyperfine splitting of the  $m_S = \{-1/2, +1/2\}$  subspace of the quartet silicon vacancy.

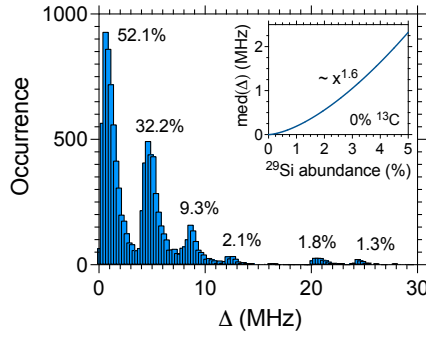


FIG. 3. Distribution of the hyperfine splitting  $\Delta$  of the  $m_S = \{-1/2, +1/2\}$  subspace of the quartet electron spin in natural abundance. The inset depicts the variation of the median of the hyperfine splitting distribution as a function of the paramagnetic  $^{29}\text{Si}$  abundance.

In Fig. 3(a), we depict the distribution of the maximal hyperfine splitting  $\sum_k A_{0k,z}$  obtained in an ensemble of  $10^4$  random nuclear spin bath configurations of natural isotope abundance. There are several peaks in the probability distribution of the maximal hyperfine splitting. The largest peak on the left corresponds to configurations with no first and second nearest neighbour nuclear spins. Going from left to right the second, third, and fourth peaks include configurations with one, two, and three second nearest neighbour  $^{29}\text{Si}$  nuclear spins. This series continues with vanishing peak heights. Furthermore, there are two additional noticeable peaks beyond 20 MHz that correspond to one  $^{13}\text{C}$  and zero  $^{29}\text{Si}$  nuclear spin and one  $^{13}\text{C}$  and one  $^{29}\text{Si}$  nuclear spins in the first and second neighbourhood shell of the silicon vacancy.

To study the nuclear spin abundance dependence of the hyperfine interaction induced local inhomogeneity we take the median of the distribution, for which we obtain 3.97 MHz in natural abundance. We note that a single value cannot properly characterize a multi peak distribution observed in Fig. 3(a), however, in paramagnetic isotope depleted samples the amplitude of the peaks beyond the first peak are significantly reduced and the distribution converges to a single peak-asymmetric distribution. In such cases, the median is a good measure of the distribution of the maximal hyperfine splitting. The median as a function of the  $^{29}\text{Si}$  abundance is depicted in Fig. 3(b). As can be seen, the median of the hyperfine splitting polynomially approaches zero as the paramagnetic silicon isotopes are depleted.

Combining our results presented so far, we conclude that the isotope purification reduces the inhomogeneous splitting of the qubit states, see Fig. 3(b), which in turn can enhance the coupling and cross-relaxation effects between the quartet silicon vacancy spin states and spin-1/2 defects in the local environment, see Fig. 2(b). This counterintuitive phenomena may lead to a drastically reduced spin state lifetime that sets the maximum for the coherence time. To quantify this effect, we calculate the spin relaxation time  $T_1$  of the

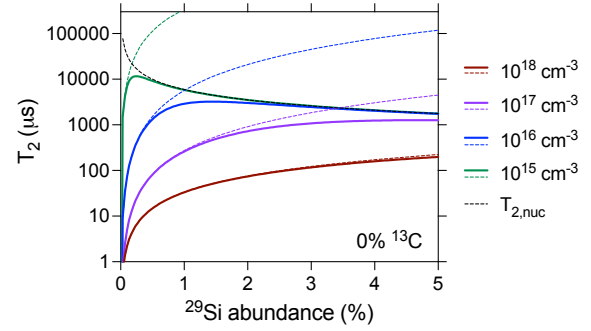


FIG. 4. Paramagnetic  $^{29}\text{Si}$  abundance dependence of the spin coherence time at various spin-1/2 point defect concentrations.  $T_{2,\text{nuc}}$  (dashed black line) is obtained at 200 G by including  $^{29}\text{Si}$  nuclear spins in the environment only. The theoretical maximum of the coherence time  $T_{2,\text{max}}$  is set by spin relaxation due to electron spins (plotted by colored dashed lines). The coherence time  $T_2$  is obtained by combining these effects (colored thick solid lines).

$|+1/2\rangle$  state the silicon vacancy as a function of the  $^{29}\text{Si}$  abundance for various spin-1/2 paramagnetic point defect concentrations. The hyperfine interaction induced local inhomogeneity, i.e. the first term on the r.h.s. of Eq. (3), is approximated by an inhomogeneous magnetic field acting on the silicon vacancy and splits the  $m_S = \{-1/2, +1/2\}$  subspace by  $\Delta = \text{median}(\sum_k A_{0k,z})$ , see Fig. 3(b). We define the absolute maximum of the coherence time as  $T_{2,\text{max}} = 2T_1$ . Here, we note that in experiments  $T_{2,\text{max}} \approx 0.5T_1$  is found for the NV center[9], therefore our results can be considered as an upper bound. To obtain the coherence time when both nuclear spins and electron spins are included in the local environment of the silicon vacancy, we use the  $T_2^{-1} = T_{2,\text{max}}^{-1} + T_{2,\text{nuc}}^{-1}$  relation, where the last term accounts for decoherence effects due to nuclear spin flip-flops induced magnetic fluctuations. Finally, we note that direct calculation of the  $T_2$  time with the gCCE method provides inaccurate results in this case, as this method substantially overestimates relaxation effects of strongly coupled spin systems[43].

The results on the ensemble averaged coherence time are depicted in Fig. 4. As can be seen the coherence time can be significantly reduced both by the increase of the electron spin concentration and the depletion of the paramagnetic isotopes. In high spin-1/2 defect concentration ( $\approx 10^{18} \text{ cm}^{-3}$ ) the  $T_2$  is maximized by the paramagnetic defects and cannot reach higher than  $\approx 100 \mu\text{s}$ . As the defect concentration reduces, the theoretical maximum of the coherence time rapidly increases and the fluctuation of the nuclear spin bath starts to limit the coherence time in natural abundance, see the calculated  $T_2$  time at, for instance, natural abundance of  $^{29}\text{Si}$  isotope in Fig. 4. Isotope purification not only reduces magnetic field fluctuations but also enhances cross relaxation effects that may become the major limiting factor in the coherence time in nuclear spin depleted samples, see Fig. 4. We note that even a very low concentration of spin-1/2 defect may have a dramatic effect on the coherence time in highly isotope

purifies samples.

Very recently a nanophotonic device integrating V2 qubit with excellent spin properties was realized in Ref. [27]. The spin coherence time was found to be 1.39 ms in a high purity isotope purified sample. The isotope abundance of the sample was estimated to be  $^{28}\text{Si} > 99.85\%$  and  $^{12}\text{C} > 99.98\%$ . Considering only magnetic field fluctuations due to the residual nuclear spin bath ( $\sim 0.15\%$   $^{29}\text{Si}$ ), we would expect a coherence time close to 25 ms. The order of magnitude difference indicates that the coherence time is limited by an effect other than nuclear spin flip-flops. Based on our results, interaction with electron spins in the lattice is a possible source of decoherence in this experiment.

Our qualitative and quantitative results are obtained for the quartet silicon vacancy in SiC. However, the spin Hamiltonian and the results in Fig. 2 can be straightforwardly generalized to spin-1 point defect qubits interacting with other spin-1 environmental defects. In this case one can also observe nearly degenerate spin states that are coupled by the dipolar interaction. For spin-1 defects not only the inhomogeneous hyperfine interaction, but also the differences of the ZFS can contribute to the splitting of the coupled states and suppress cross relaxation effects. Relaxation of the spin states is the most efficient when nearby spin-1 defects of the same kind are coupled to each other, i.e. their ZFS parameters are the same.

## ACKNOWLEDGMENTS

We acknowledge support from the Knut and Alice Wallenberg Foundation through WBSQD2 project (Grant No. 2018.0071). Support from the Swedish Government Strategic Research Area SeRC and the Swedish Government Strategic Research Area in Materials Science on Functional Materials at Linköping University (Faculty Grant SFO-Mat-LiU No. 2009 00971) is gratefully acknowledged. N. T. S. acknowledges the support from the Swedish Research Council (Grant No. VR 2016-04068), the EU H2020 project QuanTELCO (Grant No. 862721). The calculations were performed on resources provided by the Swedish National Infrastructure for Computing (SNIC) at the National Supercomputer Centre (NSC).

---

\* viktor.ivady@liu.se

- [1] G. Balasubramanian, P. Neumann, D. Twitchen, M. Markham, R. Kolesov, N. Mizuochi, J. Isoya, J. Achard, J. Beck, J. Tissler, V. Jacques, P. R. Hemmer, F. Jelezko, and J. Wrachtrup, “Ultra-long spin coherence time in isotopically engineered diamond,” *Nat. Mater.* **8**, 383 (2009).
- [2] David J. Christle, Abram L. Falk, Paolo Andrich, Paul V. Klimov, Jawad Ul Hassan, Nguyen T. Son, Erik Janzén, Takeshi Ohshima, and David D. Awschalom, “Isolated electron spins in silicon carbide with millisecond coherence times,” *Nat. Mater.* **14**, 160–163 (2015).
- [3] D. Simin, H. Kraus, A. Sperlich, T. Ohshima, G. V. Astakhov, and V. Dyakonov, “Locking of electron spin coherence above 20 ms in natural silicon carbide,” *Physical Review B* **95**, 161201 (2017), publisher: American Physical Society.
- [4] J. R. Weber, W. F. Koehl, J. B. Varley, A. Janotti, B. B. Buckley, C. G. Van de Walle, and D. D. Awschalom, “Quantum computing with defects,” *PNAS* **107**, 8513–8518 (2010).
- [5] C. L. Degen, F. Reinhard, and P. Cappellaro, “Quantum sensing,” *Rev. Mod. Phys.* **89**, 035002 (2017).
- [6] David D. Awschalom, Ronald Hanson, Jörg Wrachtrup, and Brian B. Zhou, “Quantum technologies with optically interfaced solid-state spins,” *Nature Photonics* **12**, 516–527 (2018), number: 9 Publisher: Nature Publishing Group.
- [7] L. Childress, M. V. Gurudev Dutt, J. M. Taylor, A. S. Zibrov, F. Jelezko, J. Wrachtrup, P. R. Hemmer, and M. D. Lukin, “Coherent dynamics of coupled electron and nuclear spin qubits in diamond,” *Science* **314**, 281–285 (2006).
- [8] N. Mizuochi, P. Neumann, F. Remp, J. Beck, V. Jacques, P. Siyushev, K. Nakamura, D. J. Twitchen, H. Watanabe, S. Yamasaki, F. Jelezko, and J. Wrachtrup, “Coherence of single spins coupled to a nuclear spin bath of varying density,” *Phys. Rev. B* **80**, 041201 (2009).
- [9] N. Bar-Gill, L. M. Pham, A. Jarmola, D. Budker, and R. L. Walsworth, “Solid-state electronic spin coherence time approaching one second,” *Nature Communications* **4**, 1743 (2013).
- [10] T. Yamamoto, T. Umeda, K. Watanabe, S. Onoda, M. L. Markham, D. J. Twitchen, B. Naydenov, L. P. McGuinness, T. Teraji, S. Koizumi, F. Dolde, H. Fedder, J. Honert, J. Wrachtrup, T. Ohshima, F. Jelezko, and J. Isoya, “Extending spin coherence times of diamond qubits by high-temperature annealing,” *Phys. Rev. B* **88**, 075206 (2013).
- [11] E. D. Herbschleb, H. Kato, Y. Maruyama, T. Danjo, T. Makino, S. Yamasaki, I. Ohki, K. Hayashi, H. Morishita, M. Fujiwara, and N. Mizuochi, “Ultra-long coherence times amongst room-temperature solid-state spins,” *Nature Communications* **10**, 3766 (2019), number: 1 Publisher: Nature Publishing Group.
- [12] Christopher P. Anderson, Elena O. Glen, Cyrus Zeledon, Alexandre Bourassa, Yu Jin, Yizhi Zhu, Christian Vorwerk, Alexander L. Crook, Hiroshi Abe, Jawad Ul-Hassan, Takeshi Ohshima, Nguyen T. Son, Giulia Galli, and David D. Awschalom, “Five-second coherence of a single spin with single-shot readout in silicon carbide,” *Science Advances* **8**, eabm5912, publisher: American Association for the Advancement of Science.
- [13] Matthias Widmann, Sang-Yun Lee, Torsten Rendler, Nguyen Tien Son, Helmut Fedder, Seoyoung Paik, Li-Ping Yang, Nan Zhao, Sen Yang, Ian Booker, Andrej Denisenko, Mohammad Jamali, S. Ali Momenzadeh, Ilja Gerhardt, Takeshi Ohshima, Adam Gali, Erik Janzén, and Jörg Wrachtrup, “Coherent control of single spins in silicon carbide at room temperature,” *Nat. Mater.* **14**, 164–168 (2015).
- [14] H. Kraus, V. A. Soltamov, F. Fuchs, D. Simin, A. Sperlich, P. G. Baranov, G. V. Astakhov, and V. Dyakonov, “Magnetic field and temperature sensing with atomic-scale spin defects in silicon carbide,” *Scientific Reports* **4**, 5303 (2014), number: 1 Publisher: Nature Publishing Group.
- [15] Sang-Yun Lee, Matthias Niethammer, and Jörg Wrachtrup, “Vector magnetometry based on  $s = \frac{3}{2}$  electronic spins,” *Phys. Rev. B* **92**, 115201 (2015).
- [16] D. Simin, V. A. Soltamov, A. V. Poshakinskiy, A. N. Anisimov, R. A. Babunts, D. O. Tolmachev, E. N. Mokhov, M. Trupke, S. A. Tarasenko, A. Sperlich, P. G. Baranov, V. Dyakonov, and G. V. Astakhov, “All-optical dc nanotesla magnetometry using silicon vacancy fine structure in isotopically purified silicon car-

- bide,” *Phys. Rev. X* **6**, 031014 (2016).
- [17] Matthias Niethammer, Matthias Widmann, Sang-Yun Lee, Pontus Stenberg, Olof Kordina, Takeshi Ohshima, Nguyen Tien Son, Erik Janzén, and Jörg Wrachtrup, “Vector magnetometry using silicon vacancies in 4*h*-sic under ambient conditions,” *Phys. Rev. Applied* **6**, 034001 (2016).
- [18] A. N. Anisimov, D. Simin, V. A. Soltamov, S. P. Lebedev, P. G. Baranov, G. V. Astakhov, and V. Dyakonov, “Optical thermometry based on level anticrossing in silicon carbide,” *Sci. Rep.* **6**, 33301 (2016).
- [19] V. A. Soltamov, C. Kasper, A. V. Poshakinskiy, A. N. Anisimov, E. N. Mokhov, A. Sperlich, S. A. Tarasenko, P. G. Baranov, G. V. Astakhov, and V. Dyakonov, “Excitation and coherent control of spin qubit modes in silicon carbide at room temperature,” *Nature Communications* **10**, 1678 (2019).
- [20] Tuan Minh Hoang, Hitoshi Ishiwata, Yuta Masuyama, Yuichi Yamazaki, Kazutoshi Kojima, Sang-Yun Lee, Takeshi Ohshima, Takayuki Iwasaki, Digh Hisamoto, and Mutsuko Hatano, “Thermometric quantum sensor using excited state of silicon vacancy centers in 4H-SiC devices,” *Applied Physics Letters* **118**, 044001 (2021), publisher: American Institute of Physics.
- [21] John B. S. Abraham, Cameron Gutsell, Dalibor Todorovski, Scott Sperling, Jacob E. Epstein, Brian S. Tien-Street, Timothy M. Sweeney, Jeremiah J. Wathen, Elizabeth A. Pogue, Peter G. Brereton, Tyrel M. McQueen, Wesley Frey, B. D. Clader, and Robert Osiander, “Nanotesla Magnetometry with the Silicon Vacancy in Silicon Carbide,” *Physical Review Applied* **15**, 064022 (2021), publisher: American Physical Society.
- [22] H. Kraus, V. A. Soltamov, D. Riedel, S. Vāth, F. Fuchs, A. Sperlich, P. G. Baranov, V. Dyakonov, and G. V. Astakhov, “Room-temperature quantum microwave emitters based on spin defects in silicon carbide,” *Nat. Phys.* **10**, 157–162 (2014).
- [23] Péter Udvarhelyi, Gergő Thiering, Naoya Morioka, Charles Babin, Florian Kaiser, Daniil Lukin, Takeshi Ohshima, Jawad Ul-Hassan, Nguyen Tien Son, Jelena Vučković, Jörg Wrachtrup, and Adam Gali, “Vibronic states and their effect on the temperature and strain dependence of silicon-vacancy qubits in 4*h*-SiC,” *Phys. Rev. Applied* **13**, 054017 (2020).
- [24] Péter Udvarhelyi, Roland Nagy, Florian Kaiser, Sang-Yun Lee, Jörg Wrachtrup, and Adam Gali, “Spectrally stable defect qubits with no inversion symmetry for robust spin-to-photon interface,” *Phys. Rev. Applied* **11**, 044022 (2019).
- [25] Matthias Widmann, Matthias Niethammer, Dmitry Yu. Fedyanin, Igor A. Khramtsov, Torsten Rendler, Ian D. Booker, Jawad Ul Hassan, Naoya Morioka, Yu-Chen Chen, Ivan G. Ivanov, Nguyen Tien Son, Takeshi Ohshima, Michel Bockstedte, Adam Gali, Cristian Bonato, Sang-Yun Lee, and Jörg Wrachtrup, “Electrical Charge State Manipulation of Single Silicon Vacancies in a Silicon Carbide Quantum Optoelectronic Device,” *Nano Letters* **19**, 7173–7180 (2019).
- [26] Daniil M. Lukin, Constantin Dory, Melissa A. Guidry, Ki Youl Yang, Sattwik Deb Mishra, Rahul Trivedi, Marina Radulaski, Shuo Sun, Dries Vercruysse, Geun Ho Ahn, and Jelena Vučković, “4H-silicon-carbide-on-insulator for integrated quantum and nonlinear photonics,” *Nature Photonics* **14**, 330–334 (2020), number: 5 Publisher: Nature Publishing Group.
- [27] Charles Babin, Rainer Stöhr, Naoya Morioka, Tobias Linke-witz, Timo Steidl, Raphael Wörnle, Di Liu, Erik Hesselmeier, Vadim Vorobyov, Andrej Denisenko, Mario Hentschel, Christian Gobert, Patrick Berwian, Georgy V. Astakhov, Wolfgang Knolle, Sridhar Majety, Pranta Saha, Marina Radulaski, Nguyen Tien Son, Jawad Ul-Hassan, Florian Kaiser, and Jörg Wrachtrup, “Fabrication and nanophotonic waveguide integration of silicon carbide colour centres with preserved spin-optical coherence,” *Nature Materials* **21**, 67–73 (2022), bandiera\_abtest: a Cg\_type: Nature Research Journals Number: 1 Primary\_atype: Research Publisher: Nature Publishing Group Subject\_term: Quantum information; Quantum physics; Single photons and quantum effects Subject\_term\_id: quantum-information; quantum-physics; single-photons-and-quantum-effects.
- [28] P.G. Baranov, I.V. Il’in, E.N. Mokhov, M.V. Muzafarova, S.B. Orlinskii, and J. Schmidt, “Epr identification of the triplet ground state and photoinduced population inversion for a si-c divacancy in silicon carbide,” *JETP Letters* **82**, 441–443 (2005).
- [29] D. Riedel, F. Fuchs, H. Kraus, S. Vāth, A. Sperlich, V. Dyakonov, A. A. Soltamova, P. G. Baranov, V. A. Ilyin, and G. V. Astakhov, “Resonant addressing and manipulation of silicon vacancy qubits in silicon carbide,” *Phys. Rev. Lett.* **109**, 226402 (2012).
- [30] Roland Nagy, Matthias Niethammer, Matthias Widmann, Yu-Chen Chen, Péter Udvarhelyi, Cristian Bonato, Jawad Ul Hassan, Robin Karhu, Ivan G. Ivanov, Nguyen Tien Son, Jeronimo R. Maze, Takeshi Ohshima, Öney O. Soykal, Ádám Gali, Sang-Yun Lee, Florian Kaiser, and Jörg Wrachtrup, “High-fidelity spin and optical control of single silicon-vacancy centres in silicon carbide,” *Nature Communications* **10**, 1954 (2019).
- [31] Naoya Morioka, Charles Babin, Roland Nagy, Izel Gediz, Erik Hesselmeier, Di Liu, Matthew Joliffe, Matthias Niethammer, Durga Dasari, Vadim Vorobyov, Roman Kolesov, Rainer Stöhr, Jawad Ul-Hassan, Nguyen Tien Son, Takeshi Ohshima, Péter Udvarhelyi, Gergő Thiering, Adam Gali, Jörg Wrachtrup, and Florian Kaiser, “Spin-controlled generation of indistinguishable and distinguishable photons from silicon vacancy centres in silicon carbide,” *Nature Communications* **11**, 2516 (2020), number: 1 Publisher: Nature Publishing Group.
- [32] Jun-Feng Wang, Fei-Fei Yan, Qiang Li, Zheng-Hao Liu, Jin-Ming Cui, Zhao-Di Liu, Adam Gali, Jin-Shi Xu, Chuan-Feng Li, and Guang-Can Guo, “Robust coherent control of solid-state spin qubits using anti-Stokes excitation,” *Nature Communications* **12**, 3223 (2021), number: 1 Publisher: Nature Publishing Group.
- [33] T. Wimbauer, B. K. Meyer, A. Hofstaetter, A. Scharmann, and H. Overhof, “Negatively charged si vacancy in 4*h* sic: A comparison between theory and experiment,” *Phys. Rev. B* **56**, 7384–7388 (1997).
- [34] N. Mizuochi, S. Yamasaki, H. Takizawa, N. Morishita, T. Ohshima, H. Itoh, and J. Isoya, “Continuous-wave and pulsed epr study of the negatively charged silicon vacancy with  $s = \frac{3}{2}$  and  $C_{3v}$  symmetry in *n*-type 4*h* – SiC,” *Phys. Rev. B* **66**, 235202 (2002).
- [35] S. B. Orlinski, J. Schmidt, E. N. Mokhov, and P. G. Baranov, “Silicon and carbon vacancies in neutron-irradiated sic: A high-field electron paramagnetic resonance study,” *Phys. Rev. B* **67**, 125207 (2003).
- [36] N. Mizuochi, S. Yamasaki, H. Takizawa, N. Morishita, T. Ohshima, H. Itoh, T. Umeda, and J. Isoya, “Spin multiplicity and charge state of a silicon vacancy ( $T_{V2a}$ ) in 4*h*-sic determined by pulsed epr,” *Phys. Rev. B* **72**, 235208 (2005).
- [37] Nguyen Tien Son, Pontus Stenberg, Valdas Jokubavicius, Takeshi Ohshima, Jawad Ul Hassan, and Ivan G. Ivanov, “Ligand and hyperfine interactions at silicon vacancies in 4H-SiC,” *Journal of Physics: Condensed Matter* **31**, 195501 (2019), publisher: IOP Publishing.
- [38] Viktor Ivády, Joel Davidsson, Nguyen Tien Son, Takeshi Ohshima, Igor A. Abrikosov, and Adam Gali, “Identification



- of si-vacancy related room-temperature qubits in  $4h$  silicon carbide,” *Phys. Rev. B* **96**, 161114 (2017).
- [39] Joel Davidsson, Viktor Ivády, Rickard Armiento, Takeshi Ohshima, N. T. Son, Adam Gali, and Igor A. Abrikosov, “Identification of divacancy and silicon vacancy qubits in  $6H$ -SiC,” *Applied Physics Letters* **114**, 112107 (2019), publisher: American Institute of Physics.
- [40] N. T. Son, P. Carlsson, J. ul Hassan, B. Magnusson, and E. Janzén, “Defects and carrier compensation in semi-insulating  $4h$ -SiC substrates,” *Phys. Rev. B* **75**, 155204 (2007).
- [41] Viktor Ivády, Igor A. Abrikosov, and Adam Gali, “First principles calculation of spin-related quantities for point defect qubit research,” *npj Computational Materials* **4**, 76 (2018).
- [42] Viktor Ivády, “Longitudinal spin relaxation model applied to point-defect qubit systems,” *Phys. Rev. B* **101**, 155203 (2020).
- [43] Mykyta Onizhuk, Kevin C. Miao, Joseph P. Blanton, He Ma, Christopher P. Anderson, Alexandre Bourassa, David D. Awschalom, and Giulia Galli, “Probing the Coherence of Solid-State Qubits at Avoided Crossings,” *PRX Quantum* **2**, 010311 (2021), publisher: American Physical Society.
- [44] Oscar Bulancea-Lindvall, Nguyen T. Son, Igor A. Abrikosov, and Viktor Ivády, “Dipolar spin relaxation of divacancy qubits in silicon carbide,” *npj Computational Materials* **7**, 1–11 (2021), bandiera\_abtest: a Cc\_license\_type: cc\_by Cg\_type: Nature Research Journals Number: 1 Primary\_atype: Research Publisher: Nature Publishing Group Subject\_term: Semiconductors;Spintronics Subject\_term\_id: semiconductors;spintronics.
- [45] Li-Ping Yang, Christian Burk, Matthias Widmann, Sang-Yun Lee, Jörg Wrachtrup, and Nan Zhao, “Electron spin decoherence in silicon carbide nuclear spin bath,” *Phys. Rev. B* **90**, 241203 (2014).
- [46] Oscar Bulancea-Lindvall, Matthew T. Eiles, Nguyen Tien Son, Igor A. Abrikosov, and Viktor Ivády, “Low-field microwave-free sensors using dipolar spin relaxation of quartet spin states in silicon carbide,” *arXiv:2201.03953 [cond-mat]* (2022), arXiv: 2201.03953.
- [47] A. J. Ramsay and A. Rossi, “Relaxation dynamics of spin- $\frac{3}{2}$  silicon vacancies in  $4H$ -SiC,” *Physical Review B* **101**, 165307 (2020), publisher: American Physical Society.